DOI: 10.2195/lj_Rev_sumpf_en_201411_01
URN: urn:nbn:de:0009-14-40310

Novel calculation method for chain conveyor systems

Jens Sumpf,
Hagen Bankwitz
Klaus Nendel

Institut of Material Handling, Conveying and Plastics Engineering (ifk)
Chemnitz University of Technology

Frank Rasch

iwis antriebssysteme GmbH, Wilnsdorf

Sideflexing plastic chains are used increasingly in material handling due to their highly flexible conveying design and layout options. These systems are often equipped with so called modular belts. Due to their specific force transmission, detailed calculation methods are not yet available. In the following, a generally valid calculation approach is derived and its difference to existing solutions shown by examples.

[Material handling, chain conveyor system, modular belt, conveyor chain, chain tension force, dimensioning]

1 Introduction

Suspension chain conveyors are a type of unit load conveyors based on an infinite, revolving chain. The chain serves as both, the load carrier and the traction element. Due to versatile adaptability and layout options, many different types of goods can be conveyed. Depending on the design, either horizontal or vertical transport can be realized. The chain with its function as a traction and conveying element runs preferably in a specially designed rail made of steel or plastic and is driven by form-fitted chain sprockets.

During the last years, thermoplastic chains are used increasingly in material handling due to the following main advantages: lubrication-free and maintenance-free operation, low weight and high noise attenuation as well as efficient fabrication of chain links with complex design.

This report sets its focus particularly on three different chain types which are mainly manufactured as plastic chains: slat top chains, multiflex chains, as well as modular belts (Figure 1).

Slat top chains usually consist of single-piece chain links flexibly connected by a steel bolt. The standard design of these chains only allows for straight running operation. By increasing the hinge joint, a design with a limited sideflexing-ability can be realized. Both types are offered either as plastic or steel chains and are commonly used in the beverage industry, e.g. for conveying bottles.

Multiflex chains are characterized by a gimbal, which enables outstanding spatial mobility while possessing high mechanical strength simultaneously. Apart from the connection bolts, these chains consist entirely of plastic. Compared to slat top chains, much smaller turning radii and thus extremely flexible conveyor designs can be realized. Application areas are mainly the transport of small and medium heavy goods in clean environments (e.g. food, sanitary and pharmaceutical products, and packaging) but also in linking devices of processing machines and machine tools.

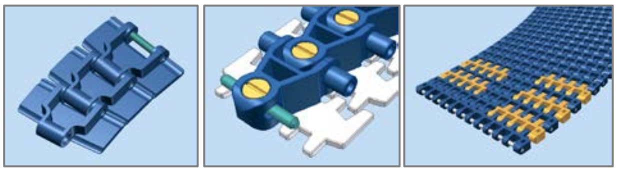

Figure 1: Slat top chain (left), multiflex chain (center) and modular belt (right)

Modular belts are conveying chains with a flat, planar geometry. They consist of individual, flexibly designed plastic modules, arranged side by side and flexibly connected in the direction of transport using plastic or steel rods. Such a construction allows realizing very wide conveyor belts. They have an accordingly broad range of application possibilities, starting with the food industry up to heavy goods transportation in the automotive sector. This type of chain can also be realized as either a straight running or a sideflexing type. The curve flexibility becomes possible by the use of a slotted hole, which enables the chain to be pushed together within the plane on the inside of the curve.

2 Known Calculation Methods and Challenges with Modular Belts

When dimensioning conveyor systems, the calculation of the chain tension forces occurring within the sys-

DOI: 10.2195/lj_Rev_sumpf_en_201411_01
URN: urn:nbn:de:0009-14-40310

tem is of great importance. The following simplified picture should aid a general understanding for the problem: In contrast to some other types of transmission systems such as flat belt or toothed belt systems, any pre-tensioning of the chain is usually not required. Therefore chain slack occurs at the lower part of the chain sprocket, where the chain tension vanishes. The force builds up slowly during the reverse movement of the chain due to its mass and the friction between the chain and the guide rail. After the reversal point has been passed, the conveying track starts. Here, the tension increases significantly due to the additional weight of the good and reaches its highest value directly before entering back into the chain sprocket.

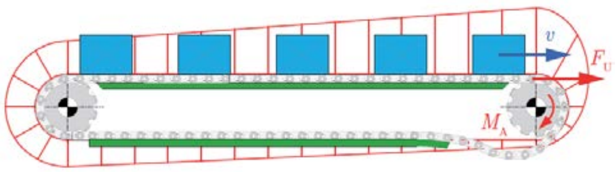

Figure 2: Simple tension force model of a chain conveyor

Calculating real conveyor systems requires at first the so called circumferential force F_U, which is the force necessary to make the chain moving. It is primarily calculated from the frictional losses at different sections of the system as well as the force to overcome slopes along the line. The circumferential force is mainly used for calculating the required driving power. Without a pre-tension force, the circumferential force, apart from some special cases, will be equal to the maximum chain tension force required for the dimensioning of the chain size or the permissible load. Often additional factors such as the startup acceleration rate have to be accounted for within the calculation.

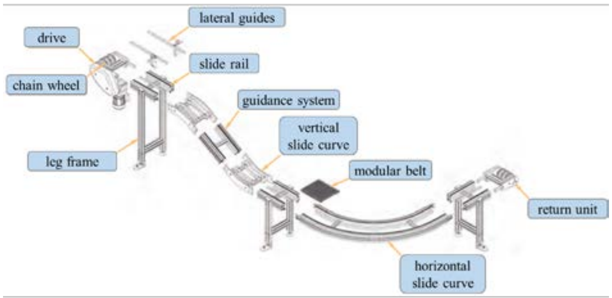

Figure 3: Schematic construction of a modular belt conveyor [Ra12], [SCH08]

The calculation of chain conveyor systems is basically identical for most cases. Starting from the chain's exit point at the drive gear, any friction and resistance forces during one revolution of the chain are summed up. Since the layout of a conveyor systems is often quite complex including flat sections, curves, slopes, buffers, etc., and having different loading conditions, the chain tension increases at a different rate within each section. Therefore the entire conveyor has to be separated into individual sections, for which distinct loading cases and calculation formulas are valid. Tracing the course of the conveyor, the exhibited chain tension force F_n at the end of a section is then the sum of the tension of the previous section $F_{\mathrm{n}-1}$ and the losses F_R of the present section due to the frictional resistance. The basic formula for calculating chain tension can thus be written as

$$F_\mathrm{n} = F_\mathrm{R} + F_{\mathrm{n}-1}. \qquad (1)$$

Most suppliers offer calculation formulas to their customers as part of their catalogues (e.g. [Int13], [Hab13], [BR12]) or in the form of a calculation program. They are usually simple and clearly structured and therefore straightforward to use.

However, the simple structure tends to be highly error-prone particularly for cases with a complex conveyor layout. On the one hand, some suppliers of conveyor systems having lower chain runs allow neglecting those respective sections in order to minimize the computational effort. On the other hand, the calculation of curved sections is often simplified in such a way that a so called curve factor is used. However, this approximation can only be shown to be valid under certain conditions [Aue06].

A first step towards a generic calculation approach has been reported by AUERBACH [Aue06]. The validity of the formulas for straight section could be confirmed and may be used generally for any conveyer system operating with traction elements such as chains, belts, etc. However, the situation is different for horizontal curves. Instead of the curve factor, the equations developed in [Aue06] are directly fed with the wrap angle as well as the friction coefficient, separated into the vertical direction (chain and good weight) and radial direction of force (curve support). This leads to significantly higher accuracy and better flexibility.

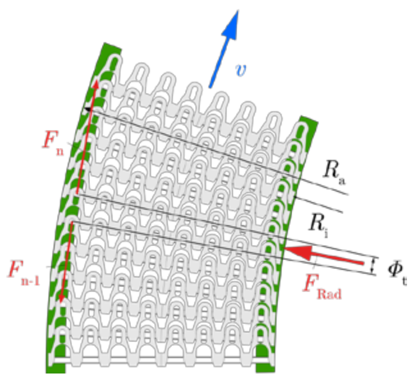

Figure 4: Transmission of chain tension and radial support for modular belts in horizontal curves

However, the validity of the equations of AUERBACH for calculating modular belts is limited by the use of an EULER-EYTELWEIN approach valid for rope wrapping. Figure 4 clearly shows an asymmetric loading of this type of chain within horizontal curves. This leads to a large distance between the point where the tension force is ex-

DOI: 10.2195/lj_Rev_sumpf_en_201411_01
URN: urn:nbn:de:0009-14-40310

erted (at the outside) and the support for the radial force (at the inside). For multiflex and slat top chains, this spatial distance is much smaller and much less important, such that omitting it in the calculation of horizontal curve section in [Aue06] yields correct results. Although this approach also shows acceptable results in the case of curved modular belts, significant deviations occur for very broad chains with a large arc of contact.

In order to correctly calculate broad conveyer systems, a novel approach is required which explicitly takes into account the extent of the traction element.

3 Load Model and Dimensioning

3.1 Straight Section

3.1.1 Loading Cases

The straight section is the most fundamental element of a conveyor system. Its calculation is mostly identical for similarly designed conveyor system based on traction elements, such as chain, belt, or toothed belt conveyors. Additionally, the equations presented in the following are mostly consistent with the calculation instructions provided by the supplier.

Simple straight section

The simplest loading case is a straight, planar section as shown in Figure 5. The load is exerted solely by the normal force F_N, which results from the good weight and the dead load of the chain. Due to the friction between chain and slide rail, this leads to the frictional force F_{RS}.

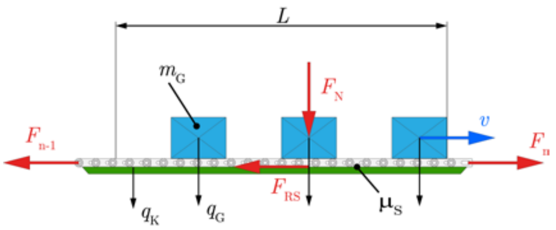

Figure 5: Simple straight section

In order to calculate the chain tension F_n at the end of the respective section according to Equation (1) (with $F_R = F_{RS}$), the tension force of the previous section F_{n-1} is used as a basis. The formula for the frictional loss F_{RS} reads as

$$F_{RS} = \mu_s \cdot g \cdot L \cdot (q_K + q_G). \qquad (2)$$

Here, μ_S is the friction coefficient between chain and rail g is the gravitational acceleration, q_G and q_K are the specific weight of the good and the chain, respectively, and L is the length of the section considered.

The specific weights of the good q_G can be found from the length of the good l_G and the distance between them l_D,

$$q_G = \frac{m_G}{(l_G + l_D)}. \qquad (3)$$

The specific weight of the chain per one meter of its length q_K can be found directly in the supplier catalog for multiflex and slat top chains. For modular belts, the supplier value m_K^* usually refers to a weight per square meter, such that it requires a multiplication by the chain width b_K:

$$q_K = m_K^* \cdot b_K. \qquad (4)$$

Straight section with slope

If the conveying section is to overcome a height difference as shown in Figure 6, the equation has to be extended by some component accounting for the slope angle.

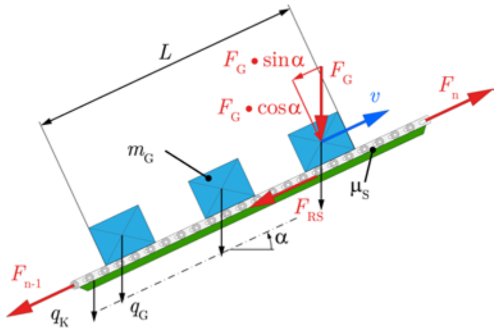

Figure 6: Straight section with slope

Therefore the chain tension force F_n will contain a component for the downhill force and can be calculated as

$$F_n = F_{RS} + F_G \cdot \sin\alpha + F_{n-1}. \qquad (5)$$

Here the force due to gravity F_G of the section can be calculated as

$$F_G = g \cdot L \cdot (q_K + q_G) \qquad (6)$$

and the friction force F_{RS} needs to be extended beyond the planar transport case (Equation (2)) by a slope factor $\cos\alpha$:

$$F_{RS} = \mu_S \cdot g \cdot L \cdot (q_K + q_G) \cdot \cos\alpha. \qquad (7)$$

Care has to be taken regarding the sign of the slope angle α. Whereas $\alpha > 0$ refers to ascending sections, a value of $\alpha < 0$ is used for descending conveying sections. By definition, the sign of α can also be found from the vertical component of the velocity vector as shown in Figure 7.

DOI: 10.2195/lj_Rev_sumpf_en_201411_01
URN: urn:nbn:de:0009-14-40310

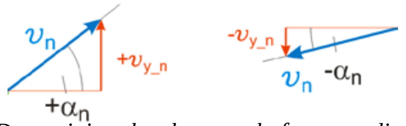

Figure 7: Determining the slope angle for ascending (left) and descending conveying sections (right)

It should be noted that Equation (5) becomes invalid if the good starts slipping on the chain if the friction coefficient is too low.

Straight section with accumulation

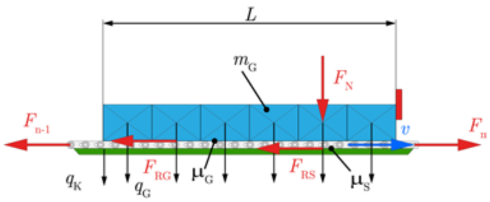

Figure 8: Straight section with accumulation

In some application cases, the conveyed good will be accumulated on the chain according to Figure 8, such that an additional friction component F_{RG} needs to be taken into account. The chain tension force F_n therefore reads as

$$F_n = F_{RS} + F_{RG} + F_{n-1} \tag{8}$$

where the friction force F_{RS} is found from Equation 2 and the friction force F_{RG} between chain and good reads as

$$F_{RG} = \mu_G \cdot g \cdot L \cdot q_G. \tag{9}$$

The friction coefficient between chain and good is described by μ_G. It should be noted that the specific good weight q_G according to Equation 3 needs to be adjusted to sections with accumulation. In such cases the distance between the pieces of goods reduces to $l_D = 0$.

Straight section with slope and accumulation

Besides the loading cases discussed before, there are situations where conveying sections may feature slope and accumulation simultaneously, as shown in Figure 9. In contrast to accumulation-free conveyance, the downhill force due to gravity is solely due to chain weight but not due to the good itself.

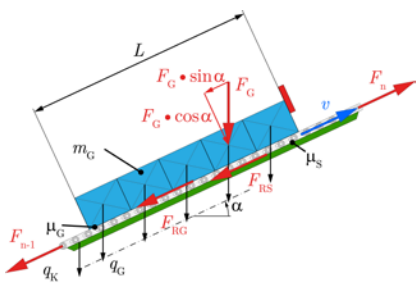

Figure 9: Straight section with slope and accumulation

The chain tension force F_n can then be calculated as

$$F_n = F_{RS} + g \cdot L \cdot q_K \cdot \sin\alpha + F_{RG} + F_{n-1} \tag{10}$$

and represents a mixture of the two previous loading cases. The friction force F_{RS} is found from Equation 7. However, for the calculation of the accumulation force F_{RG}, the good weight has to be taken into account. The equation reads as

$$F_{RG} = \mu_G \cdot g \cdot L \cdot q_G \cdot |\cos\alpha|. \tag{11}$$

3.1.2 General Equations for Straight Sections

From the loading case reviewed before, a general equation for the chain tension force of straight sections can be deduced:

$$F_n = F_{RS} + F_G \cdot \sin\alpha + F_{RG} \cdot \xi_S + F_{n-1}. \tag{12}$$

In order to distinguish between the cases where good is accumulated and where it is not, an accumulation parameter ξ_S will be introduced, defined as:

$$\text{Accumulation: } \xi_S = 1;\ \text{no accumulation: } \xi_S = 0. \tag{13}$$

The accumulation parameter is also required for the modification of Equation (6) as follows:

$$F_G = g \cdot L \cdot (q_K + q_G \cdot (1 - \xi_S)). \tag{14}$$

By virtue of Equation (7) and (11) to (14), the chain tension F_n present at the end of a straight section may now be generalized to finally read as follows:

$$F_n = g \cdot L \cdot \left[\mu_S \cdot (q_K + q_G) \cdot \cos\alpha + \left(q_K + q_G \cdot (1 - \xi_S)\right) \cdot \sin\alpha + \mu_G \cdot q_G \cdot |\cos\alpha| \cdot \xi_S\right] + F_{n-1}. \tag{15}$$

3.2 Horizontally Curved Section

3.2.1 Determining the Radial Force for Horizontal Curves

If the direction of motion is changed, the chain will also be supported at the inner part of the curve with the arc length p as shown in Figure 4. When going through the curve, friction losses occur due to the weight of the good and the weight of the chain, as discussed in the previous sections. However, additionally there are losses due to the curve friction which can be calculated from the radial support force of the chain and the friction coefficient.

DOI: 10.2195/lj_Rev_sumpf_en_201411_01
URN: urn:nbn:de:0009-14-40310

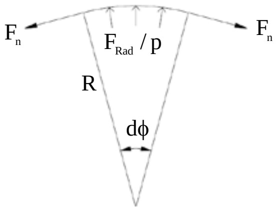

Figure 10: Arc segment

The radial force on a single chain link during a horizontal curve can be approximately calculated from the equilibrium of forces within in small arc segment (Figure 10). It follows from the equilibrium of forces in the vertical direction and some subsequent simplifications that the radial force on a chain link can be written as

$$F_{\mathrm{Rad}} = \frac{F_{\mathrm{n}}}{R} \cdot p. \tag{16}$$

3.2.2 Derivation of the Basic Equations for the Chain Tension Force

It has been demonstrated before, that modular chains are loaded inhomogeneously in the transverse direction within horizontally curved sections. Therefore the line loads f_{Ra} und f_{Ri} are introduced to aid the derivation of the equations for calculating the chain tension force. They act into the direction of chain tension and depend on the actual loading condition. By using the individual line loads, a basic equation for the calculation of the chain tension force in horizontal curves, valid for any loading case, can be derived as follows.

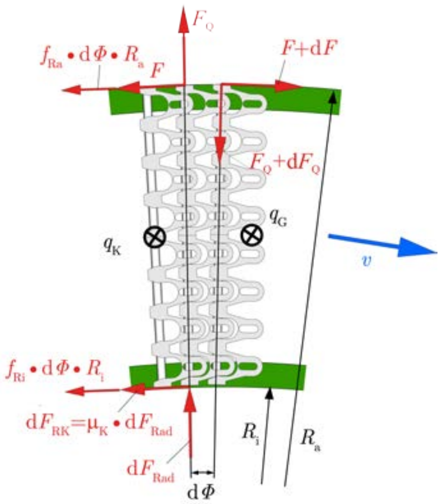

Figure 11: Differential representation of the forces within a horizontal curve

Figure 11 shows the forces of a horizontally curved section in a differential representation. The effective lengths of the line loads thereby follow from a multiplication with the angle segment under investigation and the respective radius. From the equilibrium of forces in radial direction and after some simplification one finds

$$\mathrm{d}F_{\mathrm{Rad}} - F \cdot \mathrm{d}\varphi - \mathrm{d}F_{\mathrm{Q}} = 0 \tag{17}$$

as well as from the force equilibrium in tangential direction

$$dF - F_{\mathrm{Q}} \cdot \mathrm{d}\varphi - \mathrm{d}F_{\mathrm{RK}} - f_{\mathrm{Ra}} \cdot R_{\mathrm{a}} \cdot \mathrm{d}\varphi - f_{\mathrm{Ri}} \cdot R_i \cdot \mathrm{d}\varphi = 0. \tag{18}$$

From the equilibrium of momentum around the center of the curve and subsequent simplification it follows:

$$f_{\mathrm{Ra}} \cdot R_{\mathrm{a}}^2 \cdot \mathrm{d}\varphi - \mathrm{d}F \cdot R_{\mathrm{a}} + \mu_{\mathrm{K}} \cdot \mathrm{d}F_{\mathrm{Rad}} \cdot R_{\mathrm{i}} + f_{\mathrm{Ri}} \cdot R_{\mathrm{i}}^2 \cdot \mathrm{d}\varphi + F_{\mathrm{Q}} \cdot \mathrm{d}\varphi \cdot R_{\mathrm{a}} = 0. \tag{19}$$

After solving the system of equations (Equations 17 through 19), subsequently solving the resulting system of differential equations of 1st order for the chain tension force and some final simplifications, one finds:

$$F_{\mathrm{n}}(\varphi) = (C_0 + F_{\mathrm{n-1}}) \cdot e^{C_1 \cdot \varphi} - C_0, \tag{20}$$

where the parameters C_0 and C_1 are defined as follows:

$$C_0 = \frac{f_{\mathrm{Ri}} \cdot R_{\mathrm{i}}^2 + f_{\mathrm{Ri}} \cdot R_{\mathrm{a}} \cdot R_{\mathrm{i}} + 2 \cdot f_{\mathrm{Ra}} \cdot R_{\mathrm{a}}^2}{\mu_{\mathrm{K}} \cdot (R_{\mathrm{i}} + R_{\mathrm{a}})} \tag{21}$$

$$C_1 = \frac{R_{\mathrm{a}} - \sqrt{R_{\mathrm{a}}^2 + \mu_{\mathrm{K}}^2 \cdot R_{\mathrm{a}}^2 - \mu_{\mathrm{K}}^2 \cdot R_{\mathrm{i}}^2}}{\mu_{\mathrm{K}} \cdot (R_{\mathrm{i}} - R_{\mathrm{a}})}. \tag{22}$$

As a boundary condition, homogeneously distributed line loads f_{Ra} und f_{Ri} with

$$f_{\mathrm{Ri}} = f_{\mathrm{Ra}} \cdot \frac{R_{\mathrm{a}}}{R_{\mathrm{i}}}. \tag{23}$$

is assumed, such that Equation (21) simplifies to

$$C_0 = \frac{f_{\mathrm{Ra}} \cdot R_{\mathrm{a}} \cdot (R_{\mathrm{i}} + 3 \cdot R_{\mathrm{a}})}{\mu_{\mathrm{K}} \cdot (R_{\mathrm{i}} + R_{\mathrm{a}})}. \tag{24}$$

As described above, the basic Equation (20) is valid for all horizontal curve sections. In order to investigate individual loading cases, the line load f_{Ra} has to be determined as described in Section 0 and inserted into this equation.

DOI: 10.2195/lj_Rev_sumpf_en_201411_01
URN: urn:nbn:de:0009-14-40310

3.2.3 Loading Cases for Calculating the Outer Line Load in Horizontal Curves

Simple horizontal curve

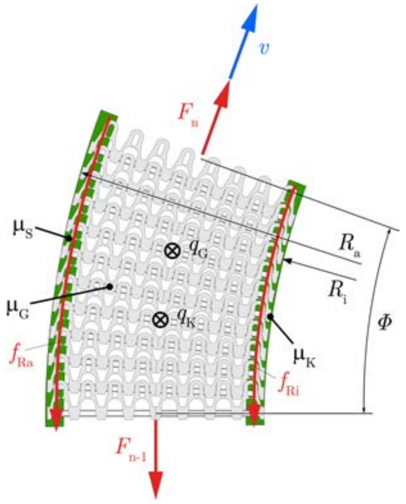

Figure 12: Schematic sketch of a horizontal curve with line load

For simple horizontal curves as shown in Figure 12, the line load f_{Ra} is determined only by the frictional force between chain and slide rail due to the specific weights of the good q_{G} and the chain q_{K} according to the relation

$$f_{\mathrm{Ra}} = \tfrac{1}{2} \cdot (q_{\mathrm{K}} + q_{\mathrm{G}}) \cdot \mu_{\mathrm{S}} \cdot g. \qquad (25)$$

Horizontal curve with accumulation

For curves subject to an additional accumulation load, the weight components known from Equation 25 have to be extended by an additional accumulation component due to the friction between chain and good with friction coefficient μ_{G}, such that the line load is calculated as

$$f_{\mathrm{Ra}} = \tfrac{1}{2} \cdot g \cdot (\mu_{\mathrm{S}} \cdot q_{\mathrm{G}} + \mu_{\mathrm{S}} \cdot q_{\mathrm{K}} + \mu_{\mathrm{G}} \cdot q_{\mathrm{G}}) \qquad (26)$$

Horizontal curve with slope

Such a loading condition can be found in conveyor systems with a so called spiral or helical shape. They are used for instance for bridging height differences in the conveying process as well as for buffering or drying/cooling of products. Due to the slope angle α, the line load f_{Ra} is then found from an appropriately adjusted frictional force based on the friction coefficient μ_{S} from the contact of chain and slide rail with the weight components of good and chain. In addition, a downhill force is created by the slope, which acts on both, the good and the chain. With those components, the equation reads as

$$f_{\mathrm{Ra}} = \tfrac{1}{2} \cdot g \cdot \big((\mu_{\mathrm{S}} \cdot \cos\alpha + \sin\alpha) \cdot q_{\mathrm{G}} + (\mu_{\mathrm{S}} \cdot \cos\alpha + \sin\alpha) \cdot q_{\mathrm{K}} \big). \qquad (27)$$

Horizontal curve with slope and accumulation

If a spiral conveyor is operated in accumulation mode, the adjusted components described before (frictional contact of good and chain as well as downhill force of the chain due to the slope angle α have to be extended by an accumulation force component due to the friction between chain and good with the friction coefficient μ_{G}. Thus the equation reads as

$$f_{\mathrm{Ra}} = \tfrac{1}{2} \cdot g \cdot \big((\mu_{\mathrm{S}} \cdot \cos\alpha + \mu_{\mathrm{G}} \cdot |\cos\alpha|) \cdot q_{\mathrm{G}} + (\mu_{\mathrm{S}} \cdot \cos\alpha + \sin\alpha) \cdot q_{\mathrm{K}} \big). \qquad (28)$$

3.2.4 General Formulation of Horizontally Curved Sections

From the four loading cases, a general formulation of the line load f_{Ra} can be found and reads as:

$$f_{\mathrm{Ra}} = \tfrac{1}{2} \cdot g \cdot \Big(\big(\mu_{\mathrm{S}} \cdot \cos\alpha + \mu_{\mathrm{G}} \cdot |\cos\alpha| \cdot \xi_S + \sin\alpha \cdot (1 - \xi_S) \big) \cdot q_{\mathrm{G}} + (\mu_{\mathrm{S}} \cdot \cos\alpha + \sin\alpha) \cdot q_{\mathrm{K}} \Big). \qquad (29)$$

This general formulation requires the accumulation parameter ξ_S as introduced in Equation (13).

3.3 Vertically Curved Sections

3.3.1 Basic Equation without Accumulation

A vertical curve can be found in those conveyor systems before and after any slope section. Such sliding curves have a similar loading as modular chains and have been already described in detail [Au06] for multiflex chains (Figure 13).

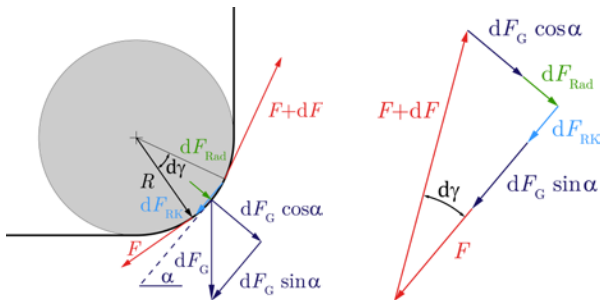

Figure 13: Schematic diagram of forces at the vertically curved section, analogous to [Aue06, S.96]

Forces exerted in vertical curves are very similar to those in horizontal curves. When analyzing a small chain section, it is obvious that the load components of radial

DOI: 10.2195/lj_Rev_sumpf_en_201411_01
URN: urn:nbn:de:0009-14-40310

force and weight are divided in different angle-dependent components at each point of the curve. By multiplication of the weight with the cosine or the sine of the angle, both components can be found analogous to the decomposition of forces at an inclined plane.

The general case of loading of a vertical curve without accumulation can be derived using Figure 13 as follows. From the equilibrium of forces in the tangential direction follows the equation in simplified form

$$\mathrm{d}F = \mathrm{d}F_{\mathrm{RK}} + \mathrm{d}F_{\mathrm{G}} \cdot \sin\alpha \tag{30}$$

with the differential changes of the force $\mathrm{d}F$, the friction force $\mathrm{d}F_{\mathrm{RK}}$ between chain and slide rail in the curve, the axial component of the force due to gravity $\mathrm{d}F_{\mathrm{G}}$ and the slope angle α. From the equilibrium of forces in the radial direction after a simplification it follows that

$$F \cdot \mathrm{d}\gamma = \mathrm{d}F_{\mathrm{Rad}} \cdot \zeta + \mathrm{d}F_{\mathrm{G}} \cdot \cos\alpha \tag{31}$$

with the differential angle-dependent force F, the differential change of the radial force $\mathrm{d}F_{\mathrm{Rad}}$ and the axial component of the force due to gravity $\mathrm{d}F_{\mathrm{G}}$. The force due to gravity of the chain section under investigation consists of the sum of specific weights of the good q_{G} and the chain q_{K}. They are multiplied by the radius of the vertical curve R, the acceleration due to gravity g, and the differential change of angle $\mathrm{d}\gamma$, which yields the equation

$$\mathrm{d}F_{\mathrm{G}} = R \cdot g \cdot (q_{\mathrm{G}} + q_{\mathrm{K}}) \cdot \mathrm{d}\gamma \tag{32}$$

The frictional force $\mathrm{d}F_{\mathrm{RK}}$ is defined as the product of the friction coefficient μ_{S} (between chain and slide rail) and the differential radial force $\mathrm{d}F_{\mathrm{Rad}}$ reading as

$$\mathrm{d}F_{\mathrm{RK}} = \mu_{\mathrm{s}} \cdot \mathrm{d}F_{\mathrm{Rad}} \cdot \zeta. \tag{33}$$

The parameter ζ describes whether the radial force of the chain points towards the center of the curve ($\zeta = 1$) or in the opposite direction ($\zeta = -1$). This distinction is required because in ascending curves the chain in certain circumstances (for example at very high goods weights) is pressed against the sliding guide at the outer radius of curvature and not against the inner curve support (see Figure 13, Figure 14 and Figure 16).

The initial value of ζ is unknown and might possibly change during the passage of ascending curves. In this case, despite a constant chain movement the direction of the frictional force would reverse suddenly. To avoid this, the product of $\mathrm{d}F_{\mathrm{Rad}} \cdot \zeta$ must always be greater than or equal to zero. That means the inequality resulting from Equation (30)

$$0 \leq F(\zeta) - \frac{\mathrm{d}F_{\mathrm{G}}}{\mathrm{d}\gamma} \cdot \cos\alpha; \quad \zeta = \begin{cases} -1 \\ 1 \end{cases} \tag{34}$$

has to be satisfied at all times. The solution of the inequality (34) has to be performed numerically.

By inserting Equation (32) as well as (33) into Equation (30) and solving for $\mathrm{d}F_{\mathrm{Rad}}$ one finds

$$\mathrm{d}F_{\mathrm{Rad}} = \frac{-(q_{\mathrm{G}} + q_{\mathrm{K}}) \cdot \mathrm{d}\gamma \cdot \sin\alpha \cdot R \cdot g + \mathrm{d}F}{\zeta \cdot \mu_{\mathrm{S}}}. \tag{35}$$

After inserting the resulting Equation (35) into (31) and solving for the force F it follows that

$$\frac{\mathrm{d}F}{\mathrm{d}\gamma} - \zeta \cdot \mu_{\mathrm{s}} \cdot F = R \cdot g \cdot (\sin\alpha - \mu_{\mathrm{s}} \cdot \cos\alpha) \cdot (q_{\mathrm{Gut}} + q_{\mathrm{Kette}}). \tag{36}$$

This obviously led again to an inhomogeneous differential equation of 1st order, as has been solved in the case of horizontal curves. For vertical curves as shown in Figure 14, the chain tension force F_{n} at the end of the curve thus yields

$$F_{\mathrm{n}} = (C_{\mathrm{G}} \cdot \cos\alpha_{n-1} + C_{\mathrm{H}} \cdot \sin\alpha_{n-1} + F_{\mathrm{n-1}}) \cdot \mathrm{e}^{\zeta \cdot \mu_{\mathrm{S}} \cdot \gamma} - C_{\mathrm{G}} \cdot \cos\alpha_n - C_{\mathrm{H}} \cdot \sin\alpha_n. \tag{37}$$

The arc angle of the curve element is denoted as γ and will be calculated as the absolute value of the difference between input and output slope angle:

$$\gamma = |\alpha_n - \alpha_{n-1}| \tag{38}$$

The constants C_{G} and C_{H} are given by the equations

$$C_{\mathrm{G}} = (q_{\mathrm{G}} + q_{\mathrm{K}}) \cdot \frac{1 - \mu_{\mathrm{S}}^2}{\mu_{\mathrm{S}}^2 + 1} \cdot R \cdot g \tag{39}$$

and

$$C_{\mathrm{H}} = (q_{\mathrm{Gut}} + q_{\mathrm{Kette}}) \cdot \frac{2 \cdot \zeta \cdot \mu_{\mathrm{s}}}{\mu_{\mathrm{S}}^2 + 1} \cdot R \cdot g \tag{40}$$

which represent the constant components of the force due to gravity (C_{G}) and the downhill force (C_{H}).

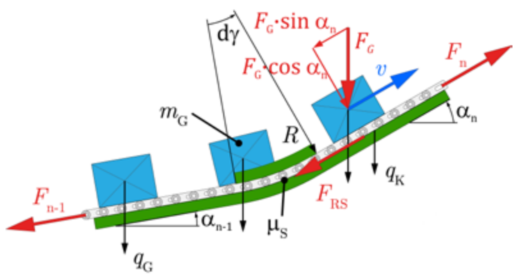

Figure 14: Ascending vertical curve

DOI: 10.2195/lj_Rev_sumpf_en_201411_01
URN: urn:nbn:de:0009-14-40310

3.3.2 Basic Equations with Accumulation

If the vertical curve is loaded by an accumulation of the goods (Figure 15), the equations are required to be adjusted to the additional accumulation force component.

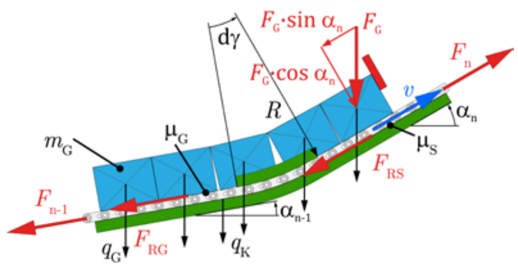

Figure 15: Ascending vertical curve with accumulation

The accumulation force can have a different sign depending on the installation position of the curve. Therefore the parameter ξ_{EB} is introduced, which will be defined as follows:

$$\xi_{EB} = \frac{\alpha_n - \alpha_{n-1}}{|\alpha_n - \alpha_{n-1}|} \tag{41}$$

The sign of the slope angle α_n and α_{n-1}, respectively, is found according to Figure 16 directly from the vertical component of the velocity vector (or the direction of motion). By using Equation (41), it follows that $\xi_{EB} = 1$ for ascending and $\xi_{EB} = -1$ for descending curves.

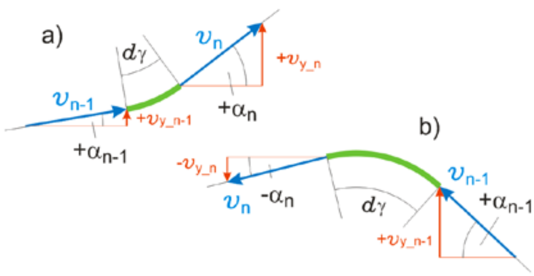

Figure 16: Determining the slope angle in vertical curves for (a) ascending and (b) descending curves.

By using the parameter ξ_{EB}, the equilibrium of forces in the tangential direction will be extended by the force component resulting from the friction coefficient μ_G between good and chain, yielding

$$\mathrm{d}F = \mathrm{d}F_{RK} + R\cdot g\cdot \mathrm{d}\gamma\cdot q_K\cdot \sin\alpha + \mu_G\cdot R\cdot g\cdot \mathrm{d}\gamma\cdot q_G\cdot \xi_{EB}\cdot \cos\alpha. \tag{42}$$

The equilibrium of forces in the radial direction corresponds to the one from Equation (31), and nothing needs to be added to the force components of Figure 13. The frictional force $\mathrm{d}F_{RK}$ between chain and the inner side of the curve is defined by Equation (33). By inserting Equations (32), (33) and (42) into each other and solving for $\mathrm{d}F_{RK}$ it follows that

$$\mathrm{d}F_{Rad} = \frac{\mathrm{d}F}{\zeta\cdot\mu_s} - \frac{(\mathrm{d}\gamma\cdot R\cdot g)\cdot(q_{Kette}\cdot\sin(\alpha))}{\zeta\cdot\mu_s} - \frac{(\mathrm{d}\gamma\cdot R\cdot g)\cdot(q_{Gut}\cdot\mu_G\cdot\xi_{EB}\cdot\cos\alpha)}{\zeta\cdot\mu_s}. \tag{43}$$

After inserting Equation (43) into (31) and solving for the force F, a differential equation is found

$$\frac{\mathrm{d}F}{\mathrm{d}\gamma} - \mu_s\cdot\zeta\cdot F = R\cdot g\cdot\big(q_{Kette}\cdot\sin\alpha + \mu_G\cdot q_{Gut}\cdot\xi_{EB}\cdot\cos\alpha - \zeta\cdot\mu_s\cdot\cos\alpha\cdot(q_{Gut}+q_{Kette})\big). \tag{44}$$

The differential equation can be solved analogously to the equation of the vertical curve without accumulation.

The calculation of the chain tension force F_n at the end of the section can be carried out similarly to the case without accumulation as shown in Equation (37). However, the constants C_G and C_H have to be adjusted to the different loading case, since they depend on the installation position for accumulation mode operation. They are given as

$$C_G = \big((\xi_{EB}\cdot\zeta\cdot\mu_s\cdot\mu_G - \mu_s^2)\cdot q_{Gut} + (1-\mu_s^2)\cdot q_{Kette}\big)\cdot\frac{R\cdot g}{\mu_s^2+1} \tag{45}$$

and

$$C_H = \big((\zeta\cdot\mu_s - \xi_{EB}\cdot\mu_G)\cdot q_{Gut} + 2\cdot\zeta\cdot\mu_s\cdot q_{Kette}\big)\cdot\frac{R\cdot g}{\mu_s^2+1}. \tag{46}$$

3.3.3 General Formulation of Vertically Curved Sections

The loading cases considered aid to find a generally valid formulation for the chain tension force for vertically curved sections. Then, Equation (37) becomes:

$$F_n = (K_G\cdot\cos\alpha_{n-1} + K_H\cdot\sin\alpha_{n-1} + F_{n-1})\cdot e^{\zeta\cdot\mu_s\cdot\gamma} - K_G\cdot\cos\alpha_n - K_H\cdot\sin\alpha_n. \tag{47}$$

The general parameters K_G and K_H with

$$K_G = \Big[\big((\xi_{EB}\cdot\zeta\cdot\mu_s\cdot\mu_G - \mu_s^2)\cdot\xi_{Stau} + (1-\mu_s^2)\cdot(1-\xi_{Stau})\big)\cdot q_{Gut} + (1-\mu_s^2)\cdot q_{Kette}\Big]\cdot\frac{\xi_{EB}\cdot R\cdot g}{\mu_s^2+1} \tag{48}$$

$$K_H = \Big[\big((\zeta\cdot\mu_s - \xi_{EB}\cdot\mu_G)\cdot\xi_{Stau} + 2\cdot\zeta\cdot\mu_s\cdot(1-\xi_{Stau})\big)\cdot q_{Gut} + 2\cdot\zeta\cdot\mu_s\cdot q_{Kette}\Big]\cdot\frac{R\cdot g}{\mu_s^2+1}. \tag{49}$$

DOI: 10.2195/lj_Rev_sumpf_en_201411_01
URN: urn:nbn:de:0009-14-40310

are deduced from both loading cases. In analogy to Section 3.1.2, the accumulation parameter ξ_S as defined by Equation (13) will be required.

3.4 Sections with Drive, Deflection, or Support Wheels

In all cases, chain conveyor systems contain drive and deflection wheels for vertical and/or horizontal curves. Occasionally, especially in the case of modular chains, there are wheels for supporting the return motion of the chain (lower chain run). Although they are usually mounted such that no relative motion is possible between the wheel and the chain, significant frictional losses may also occur here. Especially at the drive wheel or for heavy wheels in the lower chain run, strong forces on the shaft may lead to a significant friction torque.

According to Figure 17, the wrapping of a wheel will cause a force on the shaft F_W due to the chain tension force. In conjunction with the coefficient of friction in the bearing μ_W between wheel and bearing, this will lead to the frictional force F_RW.

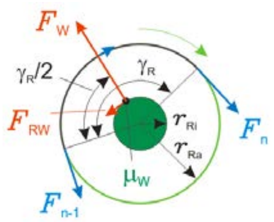

Figure 17: Wrapping of the chain around a wheel

For a defined wrap angle γ_R and by using the assumption that F_RW is relatively small, leading to an angle of the shaft force F_W of about $\gamma_R/2$, the value of F_W can be calculated approximately as

$$F_\mathrm{W} \approx 2 \cdot F_{n-1} \cdot \frac{\sin\frac{\gamma_R}{2}}{\frac{r_{Ri}}{r_{Ra}} \cdot \mu_W \cdot \sin\frac{\gamma_R}{2} - 1} \tag{50}$$

In the special case of a complete 180°-wrapping, an exact solution of F_W can be found:

$$F_\mathrm{W} = 2 \cdot \frac{F_{n-1}}{\frac{r_{Ri}}{r_{Ra}} \cdot \mu_W - 1} \tag{51}$$

From the equilibrium of momentum, and with the inside and outside radius of the pulley r_{Ri} and r_{Ra}, the chain tension force at the end of the section (when exiting the wheel) can be calculated as

$$F_\mathrm{n} = F_{n-1} + F_W \cdot \mu_W \cdot \frac{r_{Ri}}{r_{Ra}} \tag{52}$$

Supporting the chain in the lower chain run using wheels as shown in Figure 18 can be regarded as a special case. The calculation of the shaft force according to Equation (50) is not possible in that case, since the chain slack is usually unknown. In this case, a simplified estimation of F_W can be found from the chain's weight acting on the wheel, which reads as

$$F_\mathrm{W} \approx q_\mathrm{K} \cdot \frac{L_{n-1} + L_n}{2} \cdot g \tag{53}$$

For the unknown chain lengths L_{n-1} and L_n, the distances between the respective pulley and the neighboring pulleys or sections is used.

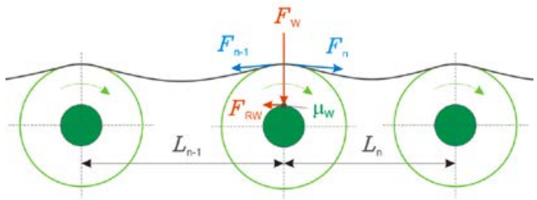

Figure 18: Chain supported by wheels

3.5 Other Losses

Besides the partial sections discussed so far, additional losses may occur in a conveyor system, e.g. wall friction, jamming of the good at the lateral support, or external forces which cannot be captured in detail. Occasionally, an elaborate and detailed calculation of certain partial sections of a system can be omitted in favor of a rough estimation of the frictional losses, if this appears to be sufficient.

In such cases it is usually convenient to introduce an external force F_{Ext} into the calculation, which leads to the following expression for the chain tension force F_n:

$$F_\mathrm{n} = F_{n-1} + F_{Ext} \tag{54}$$

3.6 Additional Steps for Dimensioning

Following the procedure above, the maximum chain tension $F_\mathrm{n\_max}$ can be calculated by summing up the individual sections. In most cases the maximum tension is located directly before the chain enters the drive sprocket. It should be noted that $F_\mathrm{n\_max}$ only contains the most significant force components due to friction and lifting, which have to be overcome by the drive motor. This tension force is also called circumferential force F_U and does not include any force components due to the pre-tension,

DOI: 10.2195/lj_Rev_sumpf_en_201411_01
URN: urn:nbn:de:0009-14-40310

since pre-tensioning is uncommon with the conveyor systems discussed. Therefore the following holds for untensioned chain conveyor systems

$$F_{n\_max} = F_U, \tag{55}$$

while for pre-tensioned systems, additional components due to the pre-tension force have to be taken into account.

For dimensioning a conveyor system, the calculated maximum chain tension force $F_{\mathrm{n\_max}}$ has to be compared with the admissible chain tension force F_{zul}^{*}. It should be noted that the calculation of $F_{\mathrm{n\_max}}$ as described before is carried out quasistatically and therefore is not able to capture all loads possible. Many suppliers therefore specify additional operational factors for particular operating conditions. Examples of such include factors for frequent start/stop events, control characteristics at start-up, velocities, as well as low or high process temperatures. The values thereof can be found in the supplier's data sheets, and the associated notes should be accounted for. Using the factors, the adjusted chain tension at the drive F_{n}^{*} and the adjusted admissible chain tension F_{zul}^{*} can be found via the relation

$$F_{\mathrm{n\_max}}^{*} \leq F_{\mathrm{zul}}^{*} \tag{56}$$

and compared to each other. If this condition is satisfied, the chain intended to be used can be considered suitable. Finally, for the dimensioning of the conveyor system, the required mechanical driving power has to be determined using the equation

$$P_{\mathrm{mech}} = F_U \cdot v \tag{57}$$

with the circumferential force F_{U} and the transport speed v.

Additional components of the conveyor system such as chain sprockets, support structures and support rollers are strongly dependent on the chain type and their eligibility has to be evaluated based on the supplier's specification.

In addition to the given mechanical layout criteria, a temperature rise due to frictional heat should be regarded as particularly critical, especially in sections with horizontal sliding curves. The heating has a strongly negative impact on the mechanical properties and the wear especially for plastic chains and plastic slide rails. It may lead to melting and the total failure of the construction element. The *ifk* of TU Chemnitz is currently developing calculation approaches for such cases.

4 Comparison of Calculation Approaches of Sliding Chain and Modular Belt Conveyors

As shown above, straight sections and slopes of modular belt conveyors including vertical curves can be calculated reliably using the existing equations for multiflex and slat top chain (e.g. according to Auerbach [Aue06]). However, the basic principle is the simplified assumption that the chain can be regarded as a rope, where the point of the force and the support merge in a single point each. Modular chains, however, show a broad transversal extent. For horizontal curves, significantly different radii of the force exertion (outside) and the support (inside) will thus occur.

Figure 19 shows a comparison between the chain tension in a conveyor system with modular belts calculated according to [Aue06] and according to the new approach. It can be easily seen that the same frictional losses result from both methods for straight sections of the curve. However, for horizontal curves, the new method shows significantly smaller losses, i.e. the conveyor will be overdesigned when using [Aue06]. Due to the exponential increase of the chain tension in such curves and the strong dependence on the force at the beginning of the curve, the largest errors occur for large wrap angles as well as at the end of the conveying sections.

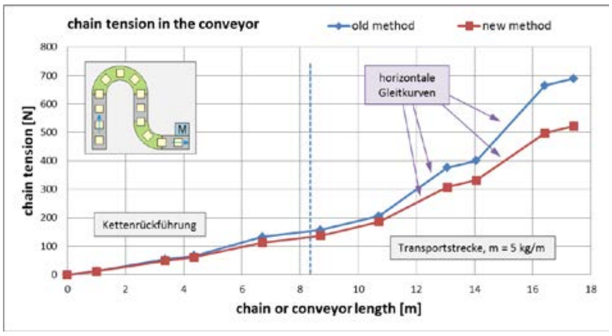

Figure 19: Comparison of the chain tension in modular belt conveyors calculated with different approaches

In the following, the influence of different parameters on the differences between the calculation approaches will be investigated. The following assumptions for a horizontal curve segment have been made and applied to the examples shown in Table 1 through Table 5, whereas one of the parameters is varied in each:

- specific weight of the chain: q_K = 5 kg/m
- chain width: b = 500 mm
- curve angle: φ = 90°
- outer curve radius*: R_a = 1000 mm
- specific weight of the good: q_G = 0 kg/m
- friction coefficient chain - rail: μ_S = μ_K = 0,25
- chain tension before the curve: F_{n-1} = 0 N

**) The outer radius is used as the basis for comparison, such that both methods use the same chain length and chain weight.*

DOI: 10.2195/lj_Rev_sumpf_en_201411_01
URN: urn:nbn:de:0009-14-40310

The results shown in Table 1 and Table 2 confirm the statement above that the most significant deviations occur for large wrap angles and large forces at the beginning of the curve. This result affects particularly long, heavily loaded, as well as winding conveying sections, e.g. as found in spiral conveyors.

Table 1: Comparison of calculation methods for horizontal curves for different curve angles

curve angle φ [°]	change of chain tension $F_n - F_{n-1}$ [N]		difference to [Aue06]
	[Aue06]	NEW	
90	23,6	21,3	-9,8%
180	58,5	47,2	-19,4%
360	187	117,1	-37,4%
720	1086	373,8	-65,6%

Table 2: Comparison of the calculation methods for horizontal curves for different forces at the beginning of the curve

chain tension F_{n-1} [N]	change of chain tension $F_n - F_{n-1}$ [N]		difference to [Aue06]
	[Aue06]	NEW	
0	23,6	21,3	-9,8%
50	47,6	32,2	-32,6%
100	71,7	43	-40%
500	264,1	129,8	-50,9%

The loading of the conveyor with goods solely affects the absolute value of the increase of the force within the curve, whereas the relative error between both methods remains constant (Table 3). Contrary to that result, a change in curve radius has no effect on the absolute value of the difference. Thus, the relative error increases for small changes of the force, as they occur for small radii (Table 4).

Table 3: Comparison of the calculation methods for horizontal curves for different good weights

specific good weight q_{Gut} [kg/m]	change of chain tension $F_n - F_{n-1}$ [N]		difference to [Aue06]
	[Aue06]	NEW	
0	23,6	21,3	-9,8%
5	47,2	42,6	-9,8%
10	70,8	63,9	-9,8%

Table 4: Comparison of calculation methods for horizontal curves for different curve radii

outer radius R_a [mm]	change of chain tension $F_n - F_{n-1}$ [N]		difference to [Aue06]
	[Aue06]	NEW	
750	17,7	15,4	-12,8%
1000	23,6	21,3	-9,8%
1500	35,4	33	-6,7
3000	70,8	68,4	-3,4

The influence of the friction coefficient should not be underestimated. The error in the calculation increases with an increasing radial friction coefficient μ_K (Table 5). On the other hand, the relative error is not affected by the friction coefficient between chain and vertical slide rail μ_S.

Table 5: Comparison of calculation methods for horizontal curves for different friction coefficients chain – slide rail

curve friction μ_K [1]	change of chain tension $F_n - F_{n-1}$ [N]		difference to [Aue06]
	[Aue06]	NEW	
0,1	20,9	20	-3,9%
0,25	23,6	21,3	-9,8%
0,4	26,8	22,6	-15,6%

5 Conclusion

In this paper, a derivation of a general calculation approach for sideflexing chain conveyer systems has been presented. One of the bases of this work was the work of Auerbach [Aue06] on the calculation of narrow chain systems. By taking into account the chain width, an improvement has been achieved which allows considering different radii which the force is acting on, as well as the radial support for horizontal redirections.

The new equations are particularly beneficial especially for conveyor systems with modular belts, where up to

DOI: 10.2195/lj_Rev_sumpf_en_201411_01
URN: urn:nbn:de:0009-14-40310

now the dimensioning could be highly error-prone under certain conditions. However, narrow chains such as slat top or multiflex chains can still be calculated using the method by setting the chain width $b_K = 0$. For this special case the results are equal to [Aue06].

In addition, the basic calculations have been extended by sections with edges as well as external forces, which were not integrated so far.

Due to the multitude of load cases possible within straight and curved sections of the conveyor system, a calculation by hand becomes highly complicated, especially for complex layouts. Therefore, the use of a computer is advisable. For this purpose, the equations for different sections were combined into single formulas, which may be easily implemented into a PC program.

REFERENCES

[Aue06] Auerbach, Peter: Zur Beanspruchung und Lebensdauer raumgängiger Gleitketten aus Kunststoffen, Technische Universität Chemnitz, Diss., 2006.

[BR12] Bosch Rexroth AG (Hrsg.): Kettenfördersysteme - VarioFlow. Ausgabe 4.4, 2012, Internet Download www.boschrexroth.com, 03.09.2013.

[Hab13] Habasit AG (Hrsg.): Technischer Leitfaden - HabasitLINK - Modularbänder. Internet Download www.habasit.com, 03.09.2013.

[Int13] Intralox, L.L.C. Europe (Hrsg.): Konstruktionshandbuch für Förderbänder, Ausgabe 2013.

[Ra12] Rasch, F.: Reibungsminderung an Stütz- und Führungselementen für Kunststoffketten. Diss. TU Chemnitz. Verlag Dr. Hut, 2012, ISBN 978-3-8439-0574-9.

[Sch08] Schüco International KG (Hrsg.): Transporttechnik, Bestell- und Fertigungskatalog 4.0, Ausgabe 2008.

Dr.-Ing. Jens Sumpf, Group Leader „Traction Mechanisms and Tribology“, Institute of Material Handling, Conveying and Plastics Engineering, Chemnitz University of Technology.

Phone: +49 371 531-32853
E-Mail: jens.sumpf@mb.tu-chemnitz.de
Web: www.gleitketten.de

Dr.-Ing. Hagen Bankwitz, Scientific Assistant, Institute of Material Handling, Conveying and Plastics Engineering, Chemnitz University of Technology.

Phone: +49 371 531-37529
E-Mail: hagen.bankwitz@mb.tu-chemnitz.de
Web: www.gleitketten.de

Prof. Dr.-Ing. Klaus Nendel, Head of Department, Institute of Material Handling, Conveying and Plastics Engineering, Chemnitz University of Technology.

Phone: +49 371 531-32323
E-Mail: klaus.nendel@mb.tu-chemnitz.de
Web: www.tu-chemnitz.de/mb/FoerdTech

Dr.-Ing. Frank Rasch, Manager Flat Top Chains, iwis antriebssysteme GmbH, Wilnsdorf.

Phone: +49 2739 86-70
E-Mail: frank.rasch@iwis.com
Web: www.iwis.com